Growth, characterization and theoretical analysis of α-$SrGeO_3$ as a candidate mid-IR stimulated Raman scattering crystal

Hailong Wang, Bin Li, Ying Zhou, Guimei Zheng, Xue Zhang and Songming Wan

Table of Contents

Synthesis of polycrystalline raw materials for growth of the α-$SrGeO_3$ crystal

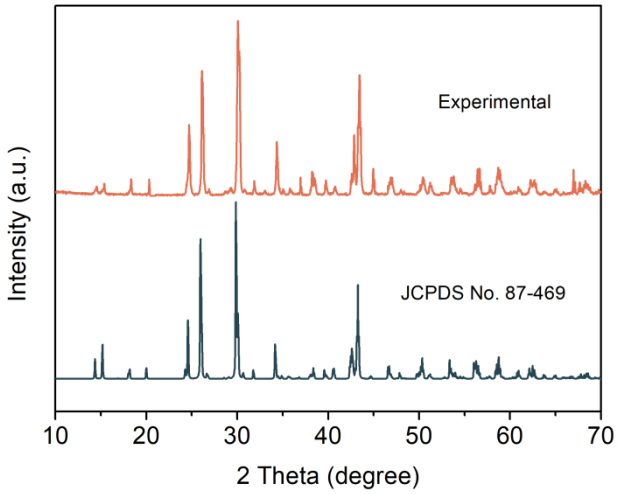

Fig. S1 Experimental and standard patterns of α-$SrGeO_3$ [Joint Committee on Powder Diffraction Standards (JCPDS) card No. 87-469].

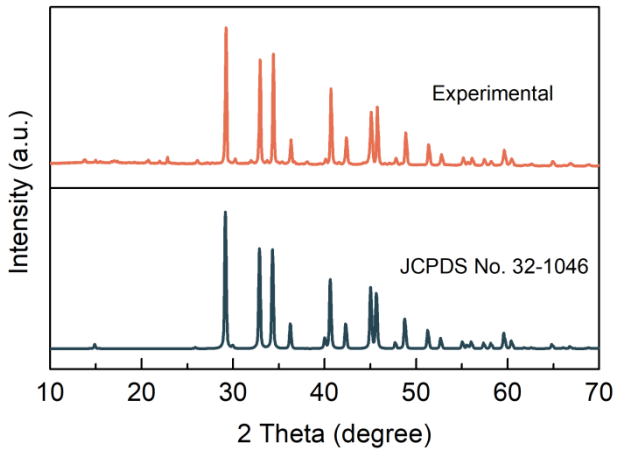

Fig. S2 Experimental and standard patterns of $NaBO_2$ (JCPDS No. 32-1046).

Polycrystalline raw materials of α-$SrGeO_3$ and $NaBO_2$ were synthesized via high-temperature solid-state reactions. All of the chemical reagents were commercially available and used without further treatment: (1) $SrCO_3$, 99.0%, Sinopharm Chemical Reagent Co., Ltd.; (2) GeO_2, 99.99%, Xiangkang Technology Development Co., Ltd., China; (3) Na_2CO_3, 99.8%, Sinopharm Chemical Reagent Co., Ltd.; (4) H_3BO_3, 99.5%, Yunling Chemical Reagent Co., China. The chemical reagents in stoichiometric ratios were weighed, mixed, and fully ground in a mortar. Then, the mixture was transferred to a corundum crucible and heated in a furnace. For α-$SrGeO_3$, the mixture was heated at 1000°C for 24 h with an intermediate grinding. For $NaBO_2$, the mixture was heated at 600°C for the first 12 hours. Then, the obtained intermediate product was reground and calcined at 650°C for the second 12 hours.

The polycrystalline products were identified by the XRD technology. The results are shown in Figs. S1 and S2, responding to polycrystalline α-$SrGeO_3$ and $NaBO_2$, respectively. The consistency of the experimental and the standard patterns indicates that the synthesized products are α-$SrGeO_3$ and $NaBO_2$.

Table S1. Convergence test for the total energy of α-$SrGeO_3$ with respect to the *k*-point grids (the energy cutoff is fixed at 1000 eV)

k-point	total energy (eV)
1 × 1 × 1	−26906.6557
1 × 2 × 1	−26906.8228
1 × 2 × 2	−26906.8363

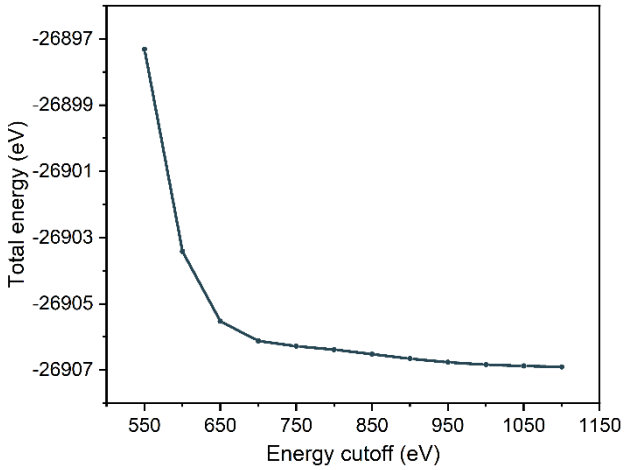

Fig. S3 Convergence test for the total energy of α-$SrGeO_3$ with respect to the energy cutoffs. The *k*-point grid is fixed at 1 × 2 × 1.

Table S1 and Fig. S3 display the results of convergence tests for the total energy of α-$SrGeO_3$ with respect to the *k*-point grids and the energy cutoffs, respectively. The results indicate that a *k*-point grid of 1 × 2 × 1 and an energy cutoff of 1000 eV are sufficient to ensure the total energy convergence to within 1 meV/atom.

Table S2. Vibrational modes and their corresponding frequencies of the α-$SrGeO_3$ crystal

No.	ω (cm^{-1})	mode	No.	ω (cm^{-1})	mode	No.	ω (cm^{-1})	mode
1	−0.03	B_u^*	31	147.52	B_u	61	360.34	A_u
2	−0.02	B_u^*	32	151.11	B_g	62	360.63	B_g
3	−0.02	A_u^*	33	154.72	B_u	63	375.14	A_g
4	65.49	B_u	34	172.10	A_u	64	376.61	B_u
5	73.79	B_g	35	176.42	B_u	65	392.33	B_u
6	78.64	A_u	36	181.01	B_g	66	423.60	B_g
7	82.40	A_u	37	192.22	B_u	67	471.68	A_u
8	84.23	B_u	38	193.25	A_g	68	473.36	A_g
9	88.77	A_g	39	195.24	A_u	69	493.50	A_g
10	94.22	B_g	40	197.11	B_g	70	494.66	B_u
11	97.51	B_g	41	243.90	A_u	71	497.05	A_u
12	98.44	A_u	42	246.69	A_g	72	498.48	B_g
13	100.51	B_u	43	254.64	A_u	73	736.43	B_u
14	103.76	B_u	44	256.09	A_g	74	740.55	B_g
15	104.39	A_g	45	262.67	B_u	75	741.98	A_g
16	109.51	A_u	46	264.34	A_u	76	744.57	A_u
17	112.76	B_u	47	265.45	B_u	77	775.75	B_g
18	113.98	B_g	48	269.10	A_u	78	775.78	B_u
19	114.05	A_g	49	270.77	A_g	79	803.59	A_g
20	119.54	B_u	50	279.63	B_g	80	805.99	B_u
21	119.97	A_u	51	281.72	B_g	81	807.40	A_u
22	121.05	B_g	52	283.42	A_g	82	816.15	A_u
23	129.32	A_g	53	302.86	B_u	83	821.40	B_g
24	132.53	A_u	54	310.57	B_g	84	821.86	A_g
25	133.96	A_g	55	312.83	A_g	85	823.30	B_u
26	137.84	B_g	56	313.03	B_u	86	850.73	B_u
27	142.62	A_u	57	316.44	A_u	87	850.91	B_g
28	142.88	B_u	58	320.24	B_g	88	852.71	A_g
29	144.93	A_g	59	354.01	A_u	89	853.37	A_u
30	145.19	B_g	60	354.53	A_g	90	883.73	B_g

*Acoustic modes

The Raman-active modes are highlighted in red.

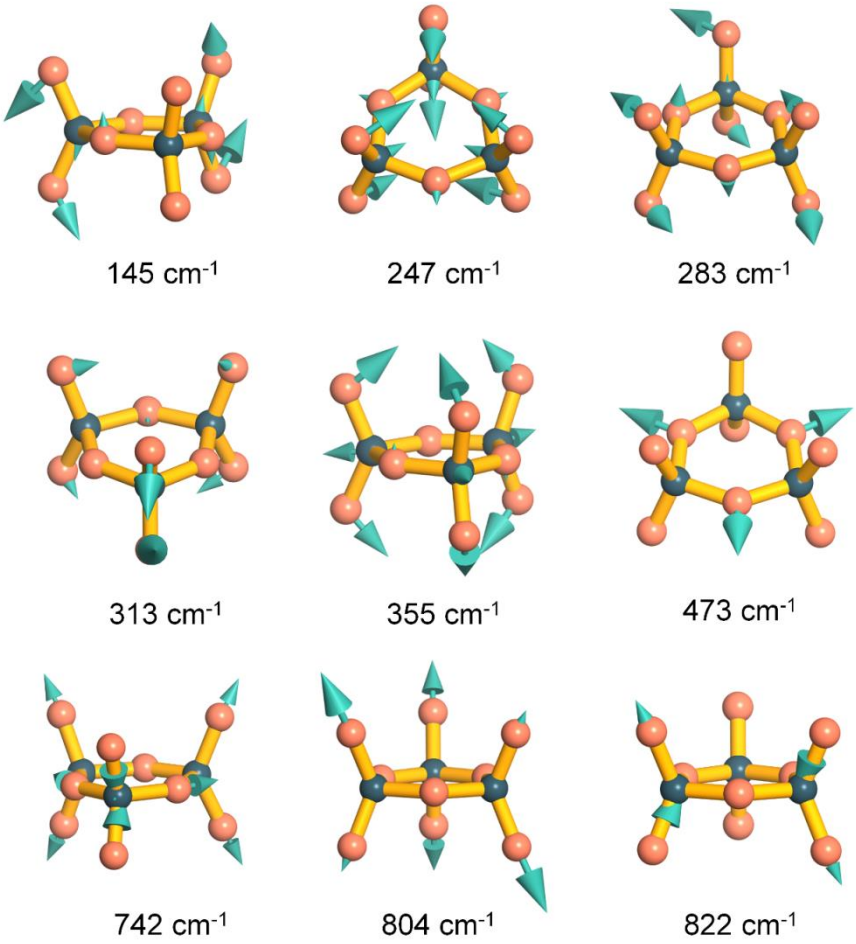

Fig. S4 Nine characteristic Raman vibrational modes of the α-$SrGeO_3$ crystal. All of the modes are the A_g mode; all of the frequencies are the computational values given in Table S2.